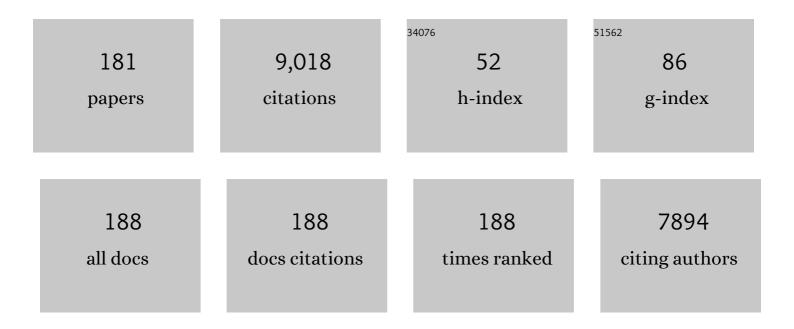
Qingfeng Ge

List of Publications by Year in descending order

Source: https://exaly.com/author-pdf/491306/publications.pdf Version: 2024-02-01



OINCEENC GE

#	Article	IF	CITATIONS
1	Active Oxygen Vacancy Site for Methanol Synthesis from CO ₂ Hydrogenation on In ₂ O ₃ (110): A DFT Study. ACS Catalysis, 2013, 3, 1296-1306.	5.5	530
2	CO2 hydrogenation to methanol over Pd/In2O3: effects of Pd and oxygen vacancy. Applied Catalysis B: Environmental, 2017, 218, 488-497.	10.8	460
3	DFT Study of CO ₂ Adsorption and Hydrogenation on the In ₂ O ₃ Surface. Journal of Physical Chemistry C, 2012, 116, 7817-7825.	1.5	265
4	Hydrogenation of CO2 to methanol over In2O3 catalyst. Journal of CO2 Utilization, 2015, 12, 1-6.	3.3	236
5	Ordering of Ruthenium Cluster Carbonyls in Mesoporous Silica. Science, 1998, 280, 705-708.	6.0	235
6	Methanol synthesis from CO2 hydrogenation over a Pd4/In2O3 model catalyst: A combined DFT and kinetic study. Journal of Catalysis, 2014, 317, 44-53.	3.1	196
7	Size Dependence of Vapor Phase Hydrodeoxygenation of <i>m</i> -Cresol on Ni/SiO ₂ Catalysts. ACS Catalysis, 2018, 8, 1672-1682.	5.5	171
8	Tribological investigation of adaptive Mo2N/MoS2/Ag coatings with high sulfur content. Surface and Coatings Technology, 2009, 203, 1304-1309.	2.2	164
9	Effect of surface hydroxyls on selective CO2 hydrogenation over Ni4/γ-Al2O3: A density functional theory study. Journal of Catalysis, 2010, 272, 227-234.	3.1	159
10	Tunability of Band Gaps in Metal–Organic Frameworks. Inorganic Chemistry, 2012, 51, 9039-9044.	1.9	148
11	Adsorption and Activation of CO over Flat and Stepped Co Surfaces:Â A First Principles Analysis. Journal of Physical Chemistry B, 2006, 110, 15368-15380.	1.2	147
12	Role of Dissociation of Phenol in Its Selective Hydrogenation on Pt(111) and Pd(111). ACS Catalysis, 2015, 5, 2009-2016.	5.5	141
13	Layered atomic structures of double oxides for low shear strength at high temperatures. Scripta Materialia, 2010, 62, 735-738.	2.6	130
14	DFT Studies of Pt/Au Bimetallic Clusters and Their Interactions with the CO Molecule. Journal of Physical Chemistry B, 2005, 109, 22341-22350.	1.2	128
15	Adsorption and Protonation of CO ₂ on Partially Hydroxylated γ-Al ₂ O ₃ Surfaces: A Density Functional Theory Study. Langmuir, 2008, 24, 12410-12419.	1.6	120
16	Mechanisms for Chain Growth in Fischer–Tropsch Synthesis over Ru(0001). Journal of Catalysis, 2002, 212, 136-144.	3.1	119
17	Effects of Hydration and Oxygen Vacancy on CO ₂ Adsorption and Activation on β-Ga ₂ O ₃ (100). Langmuir, 2010, 26, 5551-5558.	1.6	118
18	Catalytic Reduction of CO2 to CO via Reverse Water Gas Shift Reaction: Recent Advances in the Design of Active and Selective Supported Metal Catalysts. Transactions of Tianjin University, 2020, 26, 172-187.	3.3	114

#	Article	IF	CITATIONS
19	Promotional effect of surface hydroxyls on electrochemical reduction of CO2 over SnO /Sn electrode. Journal of Catalysis, 2016, 343, 257-265.	3.1	113
20	Structure Dependence of NO Adsorption and Dissociation on Platinum Surfaces. Journal of the American Chemical Society, 2004, 126, 1551-1559.	6.6	112
21	Geometric and electronic effects of bimetallic Ni–Re catalysts for selective deoxygenation of m-cresol to toluene. Journal of Catalysis, 2017, 349, 84-97.	3.1	112
22	A highly active Pt/In ₂ O ₃ catalyst for CO ₂ hydrogenation to methanol with enhanced stability. Green Chemistry, 2020, 22, 5059-5066.	4.6	107
23	Localisation of adsorbate-induced demagnetisation: CO chemisorbed on Ni{110}. Chemical Physics Letters, 2000, 327, 125-130.	1.2	102
24	Energetics, geometry and spin density of NO chemisorbed on Pt{111}. Chemical Physics Letters, 1998, 285, 15-20.	1.2	99
25	Vapor phase hydrodeoxygenation and hydrogenation of m-cresol on silica supported Ni, Pd and Pt catalysts. Chemical Engineering Science, 2015, 135, 145-154.	1.9	98
26	Direct C–C Coupling of CO ₂ and the Methyl Group from CH ₄ Activation through Facile Insertion of CO ₂ into Zn–CH ₃ σ-Bond. Journal of the American Chemical Society, 2016, 138, 10191-10198.	6.6	96
27	Interaction of Pt Clusters with the Anatase TiO2(101) Surface:Â A First Principles Study. Journal of Physical Chemistry B, 2006, 110, 7463-7472.	1.2	95
28	Understanding electronic and optical properties of anatase TiO2 photocatalysts co-doped with nitrogen and transition metals. Physical Chemistry Chemical Physics, 2013, 15, 9549.	1.3	93
29	CO2 adsorption and activation over γ-Al2O3-supported transition metal dimers: A density functional study. Catalysis Today, 2009, 147, 68-76.	2.2	91
30	Effect of PdIn bimetallic particle formation on CO 2 reduction over the Pd–In/SiO 2 catalyst. Chemical Engineering Science, 2015, 135, 193-201.	1.9	91
31	CO Adsorption on Ptâ^'Ru Surface Alloys and on the Surface of Ptâ^'Ru Bulk Alloy. Journal of Physical Chemistry B, 2001, 105, 9533-9536.	1.2	90
32	Imaging Intrinsic Diffusion of Bridge-Bonded Oxygen Vacancies onTiO2(110). Physical Review Letters, 2007, 99, 126105.	2.9	86
33	Construction of Highly Active and Selective Polydopamine Modified Hollow ZnO/Co ₃ O ₄ p-n Heterojunction Catalyst for Photocatalytic CO ₂ Reduction. ACS Sustainable Chemistry and Engineering, 2020, 8, 11465-11476.	3.2	84
34	Reverse water gas shift over In 2 O 3 –CeO 2 catalysts. Catalysis Today, 2016, 259, 402-408.	2.2	81
35	Promotion effects of Ga2O3 on CO2 adsorption and conversion over a SiO2-supported Ni catalyst. Energy and Environmental Science, 2010, 3, 1322.	15.6	80
36	Steric Effects on the Adsorption of Alkylthiolate Self-Assembled Monolayers on Au (111)â€. Journal of Physical Chemistry B, 2003, 107, 3803-3807.	1.2	78

#	Article	IF	CITATIONS
37	Structure effects on the energetic, electronic, and magnetic properties of palladium nanoparticles. Journal of Chemical Physics, 2003, 118, 5793-5801.	1.2	74
38	Imaging the Pore Structure and Polytypic Intergrowths in Mesoporous Silica. Journal of Physical Chemistry B, 1998, 102, 6933-6936.	1.2	72
39	The chemisorption and dissociation of ethylene on Pt{111} from first principles. Journal of Chemical Physics, 1999, 110, 4699-4702.	1.2	72
40	A First Principles Study of Carbonâ ´´Carbon Coupling over the {0001} Surfaces of Co and Ru. Journal of Physical Chemistry B, 2002, 106, 2826-2829.	1.2	67
41	Structure and Energetics of LiBH4and Its Surfaces: A First-Principles Studyâ€. Journal of Physical Chemistry A, 2004, 108, 8682-8690.	1.1	66
42	Unusual bridged site for adsorbed oxygen adatoms: Theory and experiment for Ir{100}–(1×2)–O. Journal of Chemical Physics, 2000, 112, 10460-10466.	1.2	65
43	Site symmetry dependence of repulsive interactions between chemisorbed oxygen atoms on Pt{100}-(1×1). Journal of Chemical Physics, 1997, 106, 1210-1215.	1.2	63
44	Correlation of adsorption energy with surface structure: ethylene adsorption on Pd surfaces. Chemical Physics Letters, 2002, 358, 377-382.	1.2	63
45	Hydrogen Adsorption on Ga ₂ O ₃ Surface: A Combined Experimental and Computational Study. Journal of Physical Chemistry C, 2011, 115, 10140-10146.	1.5	61
46	Resonant photoemission from TiO2(110) surfaces: implications on surface bonding and hybridization. Surface Science, 1996, 348, 28-38.	0.8	57
47	Studies of rhodium nanoparticles using the first principles density functional theory calculations. Chemical Physics Letters, 2002, 366, 368-376.	1.2	57
48	Effect of Surface Oxygen Vacancy on Pt Cluster Adsorption and Growth on the Defective Anatase TiO ₂ (101) Surface. Journal of Physical Chemistry C, 2007, 111, 16397-16404.	1.5	57
49	Competition and Cooperation of Hydrogenation and Deoxygenation Reactions during Hydrodeoxygenation of Phenol on Pt(111). Journal of Physical Chemistry C, 2017, 121, 12249-12260.	1.5	57
50	A density functional theory study of CO adsorption on Pt–Au nanoparticles. Computational Materials Science, 2006, 35, 247-253.	1.4	56
51	Methanol Adsorption on the Clean CeO2(111) Surface:  A Density Functional Theory Study. Journal of Physical Chemistry C, 2007, 111, 10514-10522.	1.5	56
52	ln ₂ O ₃ as a promising catalyst for CO ₂ utilization: A case study with reverse water gas shift over ln ₂ O ₃ . , 2014, 4, 140-144.		56
53	Simultaneous Activation of CH ₄ and CO ₂ for Concerted C–C Coupling at Oxide–Oxide Interfaces. ACS Catalysis, 2019, 9, 3187-3197.	5.5	56
54	An ab initio analysis of adsorption and diffusion of silver atoms on alumina surfaces. Surface Science, 2007, 601, 134-145.	0.8	55

#	Article	IF	CITATIONS
55	Interaction of Formaldehyde with the Rutile TiO ₂ (110) Surface: A Combined Experimental and Theoretical Study. Journal of Physical Chemistry C, 2016, 120, 12626-12636.	1.5	54
56	Visible-Light-Driven Multichannel Regulation of Local Electron Density to Accelerate Activation of O–H and B–H Bonds for Ammonia Borane Hydrolysis. ACS Catalysis, 2020, 10, 14903-14915.	5.5	53
57	Cooperative cobinding of synthetic and natural ligands to the nuclear receptor PPAR \hat{I}^3 . ELife, 2018, 7, .	2.8	53
58	First-principles-based kinetic Monte Carlo simulation of nitric oxide decomposition over Pt and Rh surfaces under lean-burn conditions. Molecular Physics, 2004, 102, 361-369.	0.8	50
59	Rhenium-promoted selective CO2 methanation on Ni-based catalyst. Journal of CO2 Utilization, 2018, 26, 8-18.	3.3	49
60	Titania-Modified Silver Electrocatalyst for Selective CO ₂ Reduction to CH ₃ OH and CH ₄ from DFT Study. Journal of Physical Chemistry C, 2017, 121, 16275-16282.	1.5	47
61	Surface diffusion potential energy surfaces from first principles: CO chemisorbed on Pt{110}. Journal of Chemical Physics, 1999, 111, 9461-9464.	1.2	46
62	A First-Principles Analysis of Hydrogen Interaction in Ti-Doped NaAlH4Surfaces:Â Structure and Energetics. Journal of Physical Chemistry B, 2006, 110, 25863-25868.	1.2	45
63	Dynamics of hydrogen dissociation on Pt{100}: Steering, screening and thermal roughening effects. Journal of Chemical Physics, 1997, 106, 8896-8904.	1.2	43
64	Adsorption energetics and bonding from femtomole calorimetry and from first principles theory. Advances in Catalysis, 2000, 45, 207-259.	0.1	43
65	Enhanced CO selectivity and stability for electrocatalytic reduction of CO 2 on electrodeposited nanostructured porous Ag electrode. Journal of CO2 Utilization, 2016, 15, 41-49.	3.3	43
66	Density Functional Theory Study of Methanol Decomposition on the CeO2(110) Surface. Journal of Physical Chemistry C, 2008, 112, 4257-4266.	1.5	42
67	A precursor state for formation of TiAl3 complex in reversible hydrogen desorption/adsorption from Ti-doped NaAlH4. Chemical Communications, 2006, , 1822.	2.2	40
68	First principles calculation of the energy and structure of two solid surface phases on Ir{100}. Surface Science, 1998, 418, 529-535.	0.8	36
69	Effect of Doped Transition Metal on Reversible Hydrogen Release/Uptake from NaAlH ₄ . Chemistry - A European Journal, 2009, 15, 1685-1695.	1.7	36
70	A DFT study of oxygen reduction reaction mechanism over O-doped graphene-supported Pt4, Pt3Fe and Pt3V alloy catalysts. International Journal of Hydrogen Energy, 2015, 40, 5126-5134.	3.8	36
71	Synergy between Cu and BrÃ,nsted acid sites in carbonylation of dimethyl ether over Cu/H-MOR. Journal of Catalysis, 2018, 365, 440-449.	3.1	36
72	Adsorption and activation of CO2 over the Cu–Co catalyst supported on partially hydroxylated γ-Al2O3. Catalysis Today, 2011, 165, 10-18.	2.2	35

#	Article	IF	CITATIONS
73	Selective conversion of microcrystalline cellulose into hexitols over a Ru/[Bmim]3PW12O40 catalyst under mild conditions. Catalysis Today, 2014, 233, 70-76.	2.2	33
74	Insights into the Major Reaction Pathways of Vaporâ€Phase Hydrodeoxygenation of <i>m</i> â€Cresol on a Pt/HBeta Catalyst. ChemCatChem, 2016, 8, 551-561.	1.8	33
75	Ketonization of Propionic Acid to 3-Pentanone over Ce _{<i>x</i>} Zr _{1–<i>x</i>} O ₂ Catalysts: The Importance of Acid–Base Balance. Industrial & Engineering Chemistry Research, 2018, 57, 17086-17096.	1.8	33
76	Elucidating the Structure of Bimetallic NiW/SiO ₂ Catalysts and Its Consequences on Selective Deoxygenation of <i>m</i> -Cresol to Toluene. ACS Catalysis, 2021, 11, 2935-2948.	5.5	32
77	Vacancy-Assisted Diffusion of Alkoxy Species on Rutile <mml:math xmlns:mml="http://www.w3.org/1998/Math/MathML" display="inline"><mml:msub><mml:mi>TiO</mml:mi><mml:mn>2</mml:mn></mml:msub><mml:mo stretchy="false">(<mml:mn>110</mml:mn><mml:mo) 0.784314="" 1="" 10="" 50<="" etqq1="" overlock="" rgbt="" td="" tf="" tj=""><td>2.9 567 Td (s</td><td>31 stretchy="fail</td></mml:mo)></mml:mo </mml:math 	2.9 567 Td (s	31 stretchy="fail
78	Highly efficient electrochemical hydrogenation of acetonitrile to ethylamine for primary amine synthesis and promising hydrogen storage. Chem Catalysis, 2021, 1, 393-406.	2.9	31
79	Response to "Comment on â€~Surface diffusion potential energy surfaces from first principlesâ€â€™ [J. Chem Phys. 114, 1051 (2001)]. Journal of Chemical Physics, 2001, 114, 1053.	· 1.2	30
80	A DFT study of CO2 electrochemical reduction on Pb(211) and Sn(112). Science China Chemistry, 2015, 58, 607-613.	4.2	30
81	Ketonization of Propionic Acid on Lewis Acidic Zr-Beta Zeolite with Improved Stability and Selectivity. ACS Sustainable Chemistry and Engineering, 2021, 9, 7982-7992.	3.2	30
82	Adsorption and Formation of BaO Overlayers on γ-Al ₂ O ₃ Surfaces. Journal of Physical Chemistry C, 2008, 112, 18050-18060.	1.5	29
83	Self-acceleration in the decomposition of acetic acid on Rh{111}: a combined TPD and laser induced desorption study. Surface Science, 1995, 340, 23-35.	0.8	28
84	First-Principles Analysis of NO _{<i>x</i>} Adsorption on Anhydrous γ-Al ₂ O ₃ Surfaces. Journal of Physical Chemistry C, 2009, 113, 7779-7789.	1.5	28
85	A DFT study of methanol dehydrogenation on the PdIn(110) surface. Physical Chemistry Chemical Physics, 2012, 14, 16660.	1.3	27
86	Ti3+ Defective SnS2/TiO2 Heterojunction Photocatalyst for Visible-Light Driven Reduction of CO2 to CO with High Selectivity. Catalysts, 2019, 9, 927.	1.6	27
87	Ce–UiO-66 Derived CeO ₂ Octahedron Catalysts for Efficient Ketonization of Propionic Acid. Industrial & Engineering Chemistry Research, 2020, 59, 17269-17278.	1.8	27
88	Mechanism of ozone adsorption and activation on B-, N-, P-, and Si-doped graphene: A DFT study. Chemical Engineering Journal, 2022, 430, 133114.	6.6	27
89	Insights into the Mechanism of Ozone Activation and Singlet Oxygen Generation on N-Doped Defective Nanocarbons: A DFT and Machine Learning Study. Environmental Science & Technology, 2022, 56, 7853-7863.	4.6	27
90	Imaging of Formaldehyde Adsorption and Diffusion on TiO2(110). Topics in Catalysis, 2015, 58, 103-113.	1.3	26

#	Article	IF	CITATIONS
91	Effect of Strong Metalâ€Support Interaction of Pt/TiO ₂ on Hydrodeoxygenation of mâ€Cresol. ChemistrySelect, 2018, 3, 10364-10370.	0.7	26
92	Tuning Sn-Cu Catalysis for Electrochemical Reduction of CO2 on Partially Reduced Oxides SnOx-CuOx-Modified Cu Electrodes. Catalysts, 2019, 9, 476.	1.6	26
93	CeO ₂ Facet-Dependent Surface Reactive Intermediates and Activity during Ketonization of Propionic Acid. ACS Catalysis, 2022, 12, 2998-3012.	5.5	26
94	NO monomer and (NO)x polymeric chain chemisorption on Pt{110}: Structure and energetics. Journal of Chemical Physics, 1999, 110, 12082-12088.	1.2	25
95	Lateral potential energy surfaces for molecular chemisorption on metals from experiment and theory: NO on Pt{110}-(1×2). Chemical Physics Letters, 1999, 299, 253-259.	1.2	25
96	Adsorption of CO2on Model Surfaces of Cesium Oxides Determined from First Principles. Journal of Physical Chemistry B, 2004, 108, 16798-16805.	1.2	25
97	Conversion of propionic acid and 3-pentanone to hydrocarbons on ZSM-5 catalysts: Reaction pathway and active site. Applied Catalysis A: General, 2017, 545, 79-89.	2.2	25
98	Tuning reverse water gas shift and methanation reactions during CO2 reduction on Ni catalysts via surface modification by MoOx. Journal of CO2 Utilization, 2021, 52, 101678.	3.3	25
99	Effect of Pt Clusters on Methanol Adsorption and Dissociation over Perfect and Defective Anatase TiO ₂ (101) Surface. Journal of Physical Chemistry C, 2009, 113, 20674-20682.	1.5	24
100	Insights into the Mechanism of Ammonia Decomposition on Molybdenum Nitrides Based on DFT Studies. Journal of Physical Chemistry C, 2019, 123, 554-564.	1.5	24
101	CH4 dissociation and C C coupling on Mo-terminated MoC surfaces: A DFT study. Catalysis Today, 2020, 339, 54-61.	2.2	24
102	Grain boundary sliding mechanisms in ZrN-Ag, ZrN-Au, and ZrN-Pd nanocomposite films. Applied Physics Letters, 2006, 88, 021902.	1.5	23
103	Enhanced selective deoxygenation of m-cresol to toluene on Ni/SiO2 catalysts derived from nickel phyllosilicate. Catalysis Today, 2019, 330, 149-156.	2.2	23
104	Effect of acid-metal balance of bifunctional Pt/Beta catalysts on vapor phase hydrodeoxygenation of m-cresol. Catalysis Today, 2020, 355, 43-50.	2.2	23
105	Surface kinetics of a nonlinear oxygen-induced (1×5)→(1×1) phase transition on Ir{100}. Journal of Chemical Physics, 1998, 109, 9967-9976.	1.2	22
106	Effect of γ-Al2O3 substrate on NO2 interaction with supported BaO clusters. Surface Science, 2007, 601, L65-L68.	0.8	22
107	Effect of BaO Morphology on NO _{<i>x</i>} Abatement: NO ₂ Interaction with Unsupported and I³-Al ₂ O ₃ -Supported BaO. Journal of Physical Chemistry C, 2008, 112, 16924-16931.	1.5	22
108	Effect of defects and dopants in graphene on hydrogen interaction in graphene-supported NaAlH4. International Journal of Hydrogen Energy, 2013, 38, 3670-3680.	3.8	22

#	Article	IF	CITATIONS
109	Metal-free amino-incorporated organosilica nanotubes for cooperative catalysis in the cycloaddition of CO2 to epoxides. Catalysis Today, 2019, 324, 59-65.	2.2	22
110	Tracking Site-Specific C–C Coupling of Formaldehyde Molecules on Rutile TiO ₂ (110). Journal of Physical Chemistry C, 2015, 119, 14267-14272.	1.5	21
111	Influence of Re addition to Ni/SiO2 catalyst on the reaction network and deactivation during hydrodeoxygenation of m-cresol. Catalysis Today, 2020, 347, 79-86.	2.2	21
112	Hydrogen Interaction in Ti-Doped LiBH ₄ for Hydrogen Storage: A Density Functional Analysis. Journal of Chemical Theory and Computation, 2009, 5, 3079-3087.	2.3	20
113	Enhancing tungsten oxide/SBA-15 catalysts for hydrolysis of cellobiose through doping ZrO2. Applied Catalysis A: General, 2016, 523, 182-192.	2.2	20
114	Ru supported on zirconia-modified SBA-15 for selective conversion of cellobiose to hexitols. Microporous and Mesoporous Materials, 2014, 198, 215-222.	2.2	19
115	Efficient Hydrolytic Hydrogenation of Cellulose on Mesoporous HZSM-5 Supported Ru Catalysts. Topics in Catalysis, 2015, 58, 623-632.	1.3	19
116	Low-Temperature Reductive Coupling of Formaldehyde on Rutile TiO ₂ (110). Journal of Physical Chemistry C, 2015, 119, 18452-18457.	1.5	19
117	Vapor phase hydrodeoxygenation of phenolic compounds on group 10 metal-based catalysts: Reaction mechanism and product selectivity control. Catalysis Today, 2021, 365, 143-161.	2.2	19
118	Selective CO2 hydrogenation on the γ-Al2O3 supported bimetallic Co–Cu catalyst. Catalysis Today, 2012, 194, 30-37.	2.2	18
119	Acetone-Assisted Oxygen Vacancy Diffusion on TiO ₂ (110). Journal of Physical Chemistry Letters, 2012, 3, 2970-2974.	2.1	18
120	A DFT-based study of surface chemistries of rutile TiO2 and SnO2(110) toward formaldehyde and formic acid. Catalysis Today, 2016, 274, 103-108.	2.2	18
121	Surfaceâ€Mediated Interconnections of Nanoparticles in Cellulosic Fibrous Materials toward 3D Sensors. Advanced Materials, 2020, 32, e2002171.	11.1	18
122	Thermal Conversion of Chemisorbed Acetylene to Vinylidene and Hydrogenation to Ethylidyne on Rh{111}:  A Laser Induced Desorption Study. Journal of Physical Chemistry B, 1997, 101, 1999-2005.	1.2	17
123	A first-principles study of Sc-doped NaAlH4 for reversible hydrogen storage. Journal of Alloys and Compounds, 2007, 446-447, 267-270.	2.8	17
124	Mechanistic understanding on oxygen evolution reaction on γ-FeOOH (010) under alkaline condition based on DFT computational study. Chinese Journal of Catalysis, 2017, 38, 1621-1628.	6.9	17
125	Active Site Ensembles Enabled C–C Coupling of CO ₂ and CH ₄ for Acetone Production. Journal of Physical Chemistry C, 2018, 122, 9570-9577.	1.5	17
126	Role of CO2 in the oxy-dehydrogenation of ethylbenzene to styrene on the CeO2(111) surface. Applied Surface Science, 2018, 427, 973-980.	3.1	17

#	Article	IF	CITATIONS
127	Conversion of C _{2–4} Carboxylic Acids to Hydrocarbons on HZSM-5: Effect of Carbon Chain Length. Industrial & Engineering Chemistry Research, 2019, 58, 10307-10316.	1.8	17
128	Structure, bonding, and anharmonic librational motion of CO on Ir{100}. Journal of Chemical Physics, 2002, 116, 8097-8105.	1.2	16
129	Correlation between interfacial electronic structure and mechanical properties of ZrN–Me (MeAg,) Tj ETQq1	1 0.7843 1.5	14 rgBT /0\ 16
130	Ti ³⁺ Defective TiO ₂ /CdS Z-Scheme Photocatalyst for Enhancing Photocatalytic CO ₂ Reduction to C1–C3 Products. Industrial & Engineering Chemistry Research, 2022, 61, 8724-8737.	1.8	16
131	Multilayer influences on the monolayer structure for NO on Pt{110}-(1×2). Physical Chemistry Chemical Physics, 1999, 1, 1995-2000.	1.3	15
132	Hydrogen Spillover Enhanced Hydriding Kinetics of Palladium-Doped Lithium Nitride to Lithium Imide. Journal of Physical Chemistry C, 2009, 113, 8513-8517.	1.5	15
133	Aqueous Phase Aldol Condensation of Formaldehyde and Acetone on Anatase TiO ₂ (101) Surface: A Theoretical Investigation. ChemCatChem, 2020, 12, 1220-1229.	1.8	15
134	Probing the properties of the (111) and (100) surfaces of LaB6 through infrared spectroscopy of adsorbed CO. Surface Science, 2009, 603, 3011-3020.	0.8	14
135	Effect of calcination and metal loading on the characteristics of Co/NaY catalyst for liquid-phase hydrogenation of ethyl lactate to 1,2-propanediol. Microporous and Mesoporous Materials, 2016, 233, 184-193.	2.2	14
136	Surface chemistry and reactivity of α-MoO3 toward methane: A SCAN-functional based DFT study. Journal of Chemical Physics, 2019, 151, 044708.	1.2	14
137	Polydopamine and Barbituric Acid Coâ€Modified Carbon Nitride Nanospheres for Highly Active and Selective Photocatalytic CO ₂ Reduction. European Journal of Inorganic Chemistry, 2019, 2019, 2058-2064.	1.0	14
138	A DFT study of methane conversion on Mo-terminated Mo2C carbides: Carburization vs C–C coupling. Catalysis Today, 2021, 368, 140-147.	2.2	14
139	Ru _{0.05} Ce _{0.95} O ₂ Solid Solution Derived Ru Catalyst Enables Selective Hydrodeoxygenation of mâ€Cresol to Toluene. ChemCatChem, 2021, 13, 4814-4823.	1.8	14
140	Study of the surface diffusion of CO on Pt(111) by MD simulation. Surface Science, 1994, 304, L413-L419.	0.8	13
141	The structure of carbon adsorbed on Ir{100}: LEED I–V analysis and benchmarking of DFT. Surface Science, 2001, 478, 49-56.	0.8	13
142	Balancing the Activity and Selectivity of Propane Oxidative Dehydrogenation on NiOOH (001) and (010). Transactions of Tianjin University, 2020, 26, 341-351.	3.3	13
143	CO adsorption on clean and atomic-layer-Cu-covered ZnO(101̄0) surfaces. Applied Surface Science, 1994, 82-83, 305-309.	3.1	12
144	A study of Cu growth on an yttria-stabilized ZrO2(100) surface. Thin Solid Films, 1995, 254, 10-15.	0.8	12

#	Article	IF	CITATIONS
145	Synergetic enhancement of activity and selectivity for reverse water gas shift reaction on Pt-Re/SiO2 catalysts. Journal of CO2 Utilization, 2022, 63, 102128.	3.3	12
146	Hydride-Assisted Hydrogenation of Ti-Doped NaH/Al: A Density Functional Theory Study. Journal of Physical Chemistry C, 2011, 115, 2522-2528.	1.5	11
147	First-Principles Studies on Hydrogen Desorption Mechanism of Mg _{<i>n</i>} H _{2<i>n</i>} (<i>n</i> = 3, 4). Journal of Physical Chemistry C, 2013, 117, 8099-8104.	1.5	11
148	Promoting carbon dioxide electroreduction toward ethanol through loading Au nanoparticles on hollow Cu2O nanospheres. Catalysis Today, 2021, 365, 348-356.	2.2	11
149	Characterization of surface and bulk nitrates of γ-Al2O3–supported alkaline earth oxides using density functional theory. Physical Chemistry Chemical Physics, 2009, 11, 3380.	1.3	10
150	Coverage-dependent molecular tilt of carbon monoxide chemisorbed on Pt{110}: A combined LEED and DFT structural analysis. Surface Science, 2012, 606, 383-393.	0.8	10
151	Mesoporous silica-based nanotubes loaded Pd nanoparticles: Effect of framework compositions on the performance in heterogeneous catalysis. Microporous and Mesoporous Materials, 2017, 247, 1-8.	2.2	10
152	Hollow Au-ZnO/CN Nanocages Derived from ZIF-8 for Efficient Visible-Light-Driven Hydrogen Evolution from Formaldehyde Alkaline Solution. European Journal of Inorganic Chemistry, 2019, 2019, 2761-2767.	1.0	10
153	Facile synthesis of hierarchical flower-like Ag/Cu2O and Au/Cu2O nanostructures and enhanced catalytic performance in electrochemical reduction of CO2. Frontiers of Chemical Science and Engineering, 2020, 14, 813-823.	2.3	10
154	DFT Study of Methane Activation and Coupling on the (0001) and (112Ì0) Surfaces of α- WC. Journal of Physical Chemistry C, 2020, 124, 26722-26729.	1.5	10
155	Enhanced Ethylene Formation from Carbon Dioxide Reduction through Sequential Catalysis on Au Decorated Cubic Cu ₂ O Electrocatalyst. European Journal of Inorganic Chemistry, 2021, 2021, 2353-2364.	1.0	10
156	Research Progress in Ketonization of Biomass-derived Carboxylic Acids over Metal Oxides. Acta Chimica Sinica, 2017, 75, 439.	0.5	10
157	Facile H–D exchange in adsorbed methylidyne on Pt{110}–(1×2) and deuteration to gaseous methane. Journal of Chemical Physics, 2001, 115, 11306-11316.	1.2	9
158	A DFT+U study of structure and reducibility of CenO2nâ^'x (n⩽4, 0⩽x⩽n) nanoclusters. Computatior Theoretical Chemistry, 2012, 987, 25-31.	nal and 1.1	9
159	Imaging reactions of acetone with oxygen adatoms on partially oxidized TiO2(110). Physical Chemistry Chemical Physics, 2013, 15, 13897.	1.3	9
160	Multiple light scattering and nanotip effect of hierarchical sea urchin-like W18O49 boosting photocatalytic hydrolysis of ammonia borane. International Journal of Hydrogen Energy, 2021, 46, 18964-18976.	3.8	9
161	Understanding the role of Cu ⁺ /Cu ⁰ sites at Cu ₂ O based catalysts in ethanol production from CO ₂ electroreduction -A DFT study. RSC Advances, 2022, 12, 19394-19401.	1.7	9
162	Molecular dynamics study of H2 diffusion on a Cu(111) surface. Surface Science, 1994, 301, 353-363.	0.8	8

#	Article	IF	CITATIONS
163	Catalyst size and morphological effects on the interaction of NO2 with BaO/ \hat{I}^3 -Al2O3 materials. Catalysis Today, 2010, 151, 304-313.	2.2	8
164	A density functional theory study on reduction-induced structural transformation of copper-oxide-based oxygen carrier. Journal of Chemical Physics, 2020, 152, 054709.	1.2	8
165	Oxygen Reduction Reaction Catalyzed by Pt3M (M = 3d Transition Metals) Supported on O-doped Graphene. Catalysts, 2020, 10, 156.	1.6	8
166	Inelastic scattering and chemisorption of CO on a Cu(111) surface. Surface Science, 1992, 277, 237-245.	0.8	7
167	Origin of Support Effects on the Reactivity of a Ceria Cluster. Journal of Physical Chemistry C, 2009, 113, 18296-18303.	1.5	7
168	Mechanistic Understanding of Catalytic CO2 Activation from First Principles Theory. , 2013, , 49-79.		7
169	Electrochemical reduction of CO2 at the earth-abundant transition metal-oxides/copper interfaces. Catalysis Today, 2023, 409, 53-62.	2.2	7
170	Ultrafast Preparation of Nonequilibrium FeNi Spinels by Magnetic Induction Heating for Unprecedented Oxygen Evolution Electrocatalysis. Research, 2022, 2022, .	2.8	7
171	Kinetics of ethylene conversion to ethylidyne on Rh{111} from laser-induced thermal desorption. Surface Science, 1998, 397, 13-22.	0.8	6
172	A Comparative Study of Methanol Adsorption and Dissociation over WO3(001) and ReO3(001). Topics in Catalysis, 2015, 58, 655-664.	1.3	6
173	Surface cavity effect on C2H4 formation from electrochemical reduction of CO2 as studied using Cu2O cubes. Journal of Solid State Electrochemistry, 0, , .	1.2	6
174	Effect of postsynthesis preparation methods on catalytic performance of Ti-Beta zeolite in ketonization of propionic acid. Microporous and Mesoporous Materials, 2022, 330, 111625.	2.2	5
175	Transition-Metal-Doped Aluminum Hydrides as Building Blocks for Supramolecular Assemblies. Journal of Physical Chemistry A, 2010, 114, 12318-12322.	1.1	4
176	Using first-principles metadynamics simulation to predict new phases and probe the phase transition of NaAlH ₄ . Journal of Physics Condensed Matter, 2011, 23, 345401.	0.7	3
177	Anisotropic N-Modification of the Mo ₄ Ensemble for Efficient Ammonia Synthesis on Molybdenum Nitrides. Journal of Physical Chemistry C, 2020, 124, 616-624.	1.5	3
178	Electrochemical reduction of CO ₂ to CO and HCOO ^{â^'} using metal–cyclam complex catalysts: predicting selectivity and limiting potential from DFT. Dalton Transactions, 2021, 50, 11446-11457.	1.6	3
179	Bamboo-like N-doped carbon nanotubes encapsulating M(Co, Fe)-Ni alloy for electrochemical production of syngas with potential-independent CO/H2 ratios. Frontiers of Chemical Science and Engineering, 0, , 1.	2.3	1
180	Structure and Energetics of LiBH4 and Its Surfaces: A First-Principles Study ChemInform, 2004, 35, no.	0.1	0

#	Article	IF	CITATIONS
181	Gas Surface Interaction and Surface Reactions. Springer Handbooks, 2020, , 905-928.	0.3	Ο